Radiation build-up in laminar and turbulent regimes in quasi-CW Raman fiber laser

Sergey V. Smirnov,[1] Nikita Tarasov,[2,3] and Dmitry V. Churkin[1,2,4,*]

[1]*Novosibirsk State University, 630090, Novosibirsk, Russia*
[2]*Aston Institute of Photonic Technologies, Aston University, Birmingham, B4 7ET, UK*
[3]*Institute of Computational Technologies, SB RAS, Novosibirsk 630090, Russia*
[4]*Institute of Automation and Electrometry SB RAS, 1 Ac. Koptyug ave., Novosibirsk, 630090, Russia*
[*]*novolaser@gmail.com*

Abstract: We study the radiation build-up in laminar and turbulent generation regimes in quasi-CW Raman fiber laser. We found the resulted spectral shape and generation type is defined by the total spectral broadening/narrowing balance over laser cavity round-trip, which is substantially different in different regimes starting from first round-trips of the radiation build-up. In turbulent regime, the steady-state is reached only after a few round-trips, while in the laminar regime the laser approaches the equilibrium spectrum shape asymptotically.

OCIS codes: (140.3510) Lasers, fiber; (190.4370) Nonlinear optics, fibers; (190.5650) Raman effect; (190.5890) Scattering, stimulated.

References and links

1. S. K. Turitsyn, J. D. Ania-Castañón, S. A. Babin, V. Karalekas, P. Harper, D. Churkin, S. I. Kablukov, A. E. El-Taher, E. V. Podivilov, and V. K. Mezentsev, "270-km ultralong Raman fiber laser," Phys. Rev. Lett. **103**(13), 133901 (2009).
2. S. A. Babin, D. V. Churkin, A. E. Ismagulov, S. I. Kablukov, and E. V. Podivilov, "Four-wave-mixing-induced turbulent spectral broadening in a long Raman fiber laser," J. Opt. Soc. Am. B **24**(8), 1729–1738 (2007).
3. S. I. Kablukov, E. A. Zlobina, E. V. Podivilov, and S. A. Babin, "Output spectrum of Yb-doped fiber lasers," Opt. Lett. **37**(13), 2508–2510 (2012).
4. A. Picozzi, J. Garnier, T. Hansson, P. Suret, S. Randoux, G. Millot, and D. N. Christodoulides, "Optical wave turbulence: Towards a unified nonequilibrium thermodynamic formulation of statistical nonlinear optics," Phys. Rep. **542**(1), 1–132 (2014).
5. B. Barviau, B. Kibler, and A. Picozzi, "Wave-turbulence approach of supercontinuum generation: Influence of self-steepening and higher-order dispersion," Phys. Rev. A **79**(6), 063840 (2009).
6. D. V. Churkin, I. V. Kolokolov, E. V. Podivilov, I. D. Vatnik, M. A. Nikulin, S. S. Vergeles, I. S. Terekhov, V. V. Lebedev, G. Falkovich, S. A. Babin, and S. K. Turitsyn, "Wave kinetics of random fibre lasers," Nat. Commun. **2**, 6214 (2015).
7. S. Randoux, P. Walczak, M. Onorato, and P. Suret, "Intermittency in integrable turbulence," Phys. Rev. Lett. **113**(11), 113902 (2014).
8. P. Walczak, S. Randoux, and P. Suret, "Optical rogue waves in integrable turbulence," Phys. Rev. Lett. **114**(14), 143903 (2015).
9. M. Conforti, A. Mussot, J. Fatome, A. Picozzi, S. Pitois, C. Finot, M. Haelterman, B. Kibler, C. Michel, and G. Millot, "Turbulent dynamics of an incoherently pumped passive optical fiber cavity: Quasisolitons, dispersive waves, and extreme events," Phys. Rev. A **91**(2), 023823 (2015).
10. S. Wabnitz, "Optical turbulence in fiber lasers," Opt. Lett. **39**(6), 1362–1365 (2014).
11. E. G. Turitsyna, G. Falkovich, V. K. Mezentsev, and S. K. Turitsyn, "Optical turbulence and spectral condensate in long-fiber lasers," Phys. Rev. A **80**(3), 031804 (2009).
12. E. G. Turitsyna, S. V. Smirnov, S. Sugavanam, N. Tarasov, X. Shu, S. A. Babin, E. V. Podivilov, D. V. Churkin, G. Falkovich, and S. K. Turitsyn, "The laminar–turbulent transition in a fibre laser," Nat. Photonics **7**(10), 783–786 (2013).
13. P. Suret, P. Walczak, and S. Randoux, "Transient buildup of the optical power spectrum in Raman fiber lasers," Opt. Express **21**(2), 2331–2336 (2013).
14. E. G. Turitsyna, S. K. Turitsyn, and V. K. Mezentsev, "Numerical investigation of the impact of reflectors on spectral performance of Raman fibre laser," Opt. Express **18**(5), 4469–4477 (2010).
15. D. V. Churkin, S. V. Smirnov, and E. V. Podivilov, "Statistical properties of partially coherent cw fiber lasers," Opt. Lett. **35**(19), 3288–3290 (2010).

#248319 Received 21 Aug 2015; revised 5 Oct 2015; accepted 6 Oct 2015; published 12 Oct 2015

16. D. V. Churkin and S. V. Smirnov, "Numerical modelling of spectral, temporal and statistical properties of Raman fiber lasers," Opt. Commun. **285**(8), 2154–2160 (2012).
17. R. G. Smith, "Optical power handling capacity of low loss optical fibers as determined by stimulated Raman and brillouin scattering," Appl. Opt. **11**(11), 2489–2494 (1972).
18. S. Randoux, N. Dalloz, and P. Suret, "Intracavity changes in the field statistics of Raman fiber lasers," Opt. Lett. **36**(6), 790–792 (2011).
19. P. Walczak, S. Randoux, and P. Suret, "Statistics of a turbulent Raman fiber laser," Opt. Lett. **40**(13), 3101–3104 (2015).

1. Introduction

Quasi-CW fiber lasers such as Raman fiber lasers (RFLs) and Ytterbium-doped fiber lasers (YDFLs) are well-known for generating a huge number of different longitudinal modes simultaneously. Indeed, at typical spectrum width 0.1–1 nm and typical cavity lengths starting from 10 meters for YDFL to hundreds of kilometers for RFLs [1], the total number of generation modes is varying from thousands in YDFL to hundreds of millions in RFLs. It has been shown that numerous longitudinal modes interact nonlinearly via four-wave mixing processes which could be described in different limiting cases by wave turbulence approach [2,3]. In general, approaches of the optical wave turbulence found broad implications in optics recently [4] being capable to describe the emergence of optical rogue waves, supercontinuum generation [5], random fiber lasers [6]. Recently, intermittency and rogue waves in integrable turbulence have been observed using optical fiber as a test system [7–9]. Turbulent-like generation in YDFLs could be also modeled within the Ginzburg-Landau equation [10].

It was theoretically predicted that principally different generation type from turbulent generation could be possible in quasi-CW fiber lasers – a spectral condensate [11]. Further on, the spectral condensate was experimentally observed in [12]. The corresponding generation state was called a laminar generation in analogy with fluid flows in pipes and in contrast to well known turbulent generation.

The generation properties are very different in laminar and turbulent regimes [12]. In laminar phase, the generation spectrum is narrow and consists of highly correlated modes, which results in the suppression of intensity fluctuations, while in turbulent regime the generation spectrum is broad and intensity fluctuations are substantial. This makes fibre lasers, being dissipative in their nature, behave similar to Hamiltonian systems exhibiting a condensation phenomenon [4]. Till now, it is not clear what are the mechanisms establishing a spectral condensate (laminar generation) in a fibre laser and how the same initial noise evolves into so radically different (laminar and turbulent) generation regimes under very similar parameters of the laser.

Here we take this challenge by tracking in a dynamic way how the laser relaxes into steady-state from the initial noise. For turbulent regime, the radiation build-up in was studied previously in [13,14]. In [13] it was directly measured how the spectrum becomes broader owing to turbulence induced four-wave mixing after the laser is switched on. The role of the spectral profiles of mirrors on the radiation build-up in turbulent regime is studied numerically in [14]. Till now nothing is known about how the laminar regime is building up.

In the present paper we numerically study the radiation build-up in both laminar and turbulent cases in quasi-CW Raman fiber laser and tackle different mechanisms behind the generation formation. We show that the radiation dynamics start to differentiate after initial few round-trips when the pump light is switched on. In turbulent case, the radiation exhibits strong nonlinear broadening at each cavity pass and, at the same time, strong filtering (narrowing) on laser mirrors, so the spectrum acquires some self-consistent steady shape. In laminar case, the spectrum becomes incrementally narrower at each round-trip slowly approaching its final shape over many round-trips of evolution in the laser cavity.

#248319 Received 21 Aug 2015; revised 5 Oct 2015; accepted 6 Oct 2015; published 12 Oct 2015

2. Numerical model

We consider numerically RFL following [12], Fig. 1. The laser has a single-side pumping at 1455 nm and generates at 1555 nm. The spectral, temporal and statistical properties of the generated wave are described well by the nonlinear Schrödinger equation (NLSE) [15,16]:

$$\frac{\partial A_s^{\pm}}{\partial z^{\pm}} + \frac{i}{2}\beta_{2s}\frac{\partial^2 A_s^{\pm}}{\partial t^2} + \frac{\alpha_s}{2}A_s^{\pm} = i\gamma_s\left|A_s^{\pm}\right|^2 A_s^{\pm} + \frac{g_s}{2}\left(\left\langle\left|A_p^{\pm}\right|^2\right\rangle + \left\langle\left|A_p^{\mp}\right|^2\right\rangle\right)A_s^{\pm},$$

where A is the complex field envelope, t is the time in a frame of reference moving with the pump, v_{gs} is the difference between pump and generation Stokes waves inverse group velocities, β_2, α, γ, g are the dispersion, linear attenuation, Kerr and Raman coefficients, ω stands for frequency. Sign $\pm$ denotes counter-propagating waves, "s" and "p" are used for generation and pump waves, z is the longitudinal coordinate with $z = 0$ at the starting point of propagation and $z = L$ at the other fiber end, L is the fiber length. Note that for every point of the fiber, longitudinal coordinate value z^+ for "+" wave corresponds to the value of z^- for "–" wave and vice versa. Angle brackets denote time averaging. Spontaneous Raman emission was taken into account by using white noise as an initial condition [17]. Similar NLSE describes the evolution of the pump wave. We use the following parameters: $\alpha_s = 0.83$ km^{-1}, $\alpha_p = 0.51$ km^{-1}, $\gamma_s = 2.58$ (km*W)$^{-1}$, $\gamma_p = 3.0$ (km*W)$^{-1}$, $g_s = 1.30$ (km*W)$^{-1}$, $g_p = 1.51$ (km·W)$^{-1}$, $\beta_{2p} = 17.9$ ps^2/km, $1/v_{gs} = -4.5$ ns/km, $L = 370$ m, pump power $P = 3$ W. Mirrors were modeled by super-Gaussian profile of 6th order, full width at half maximum of 1 nm, and reflectivity of 1 at spectral maximum.

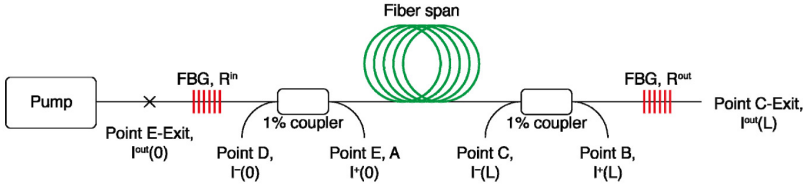

Fig. 1. Raman fiber laser setup with marked points where the generation properties are analyzed: A – initial point for the generation wave co-propagating with the pump wave, B – after propagation along the fiber, but before the reflection from the right laser mirror, C – after reflection from the laser mirror, D – after propagation in direction opposite to the pump wave.

3. Dynamics of radiation build-up in laminar and turbulent regimes

The generation properties of a laser depend on the cavity parameters, the spectral profiles of laser mirrors, and operation power: the laser can operate either in turbulent or laminar regime [12]. Here we investigate processes of radiation build-up in both regimes by fixing all cavity parameters except the value of the fiber dispersion. We use two values of the fiber dispersion: 7 ps^2/km and 35 ps^2/km. At low dispersion, the turbulent generation is established with broad generation spectrum, while in the laser with high fiber dispersion, the generation is laminar having narrow spectrum, Fig. 2(a). Note that intensity spatio-temporal dynamics and intensity probability density functions are also very different in both regimes: fluctuations are suppressed in laminar regime [12]. We also observe these features in our numerical simulations, but further we focus on spectral properties only to distinguish two regimes.

Starting from same noise conditions, the radiation evolves in different ways to the equilibrium spectrum in different generation regimes. Indeed, after first few round-trips, the spectral shape of generation spectrum repeats in general the spectral shape of laser mirrors, growing exponentially in its amplitude, Figs. 2(b) and 2(c). However, after the 5th round-trip, the spectral dynamics is substantially different in different regimes. In the turbulent regime the spectrum becomes broader while the generation wave continues to circulate in the cavity.

#248319 Received 21 Aug 2015; revised 5 Oct 2015; accepted 6 Oct 2015; published 12 Oct 2015

In the laminar regime, after initial spectral broadening stage, the spectrum starts to become gradually narrower.

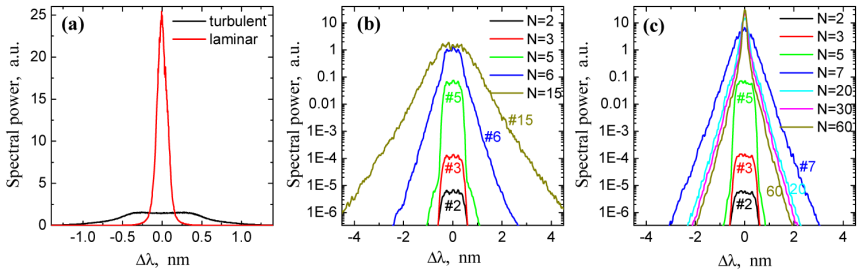

Fig. 2. (a) Optical spectrum in laminar (red) and turbulent (black) generation regimes. (b,c) The spectrum dynamics in (b) turbulent and (c) laminar regimes. N is the number of round-trips after the moment of time when the pump wave is switched on.

To study the radiation build-up in more details, we use the rms spectral width, Γ, as a measure of spectral width and calculate it at different points inside the resonator as well as track its changes over the successive cavity round-trips. In particular, we calculate the spectral width at points B and D, Γ_B and Γ_D, i.e. after each pass in the fiber before transmission through the laser mirror, and at points C and A, Γ_C and Γ_A, i.e. after the reflection from laser mirrors. Then we calculate the spectral broadening factor as a ratio Γ_B/Γ_A and Γ_D/Γ_C, which gives us the information of the impact of the propagation over the cavity fiber on spectral properties of the generation wave, Figs. 3(a) and 3(d). We also investigate the impact of cavity mirrors on spectral properties by calculating the spectral broadening factor as a ratio Γ_C/Γ_B and Γ_A/Γ_D, Figs. 3(b) and 3(e).

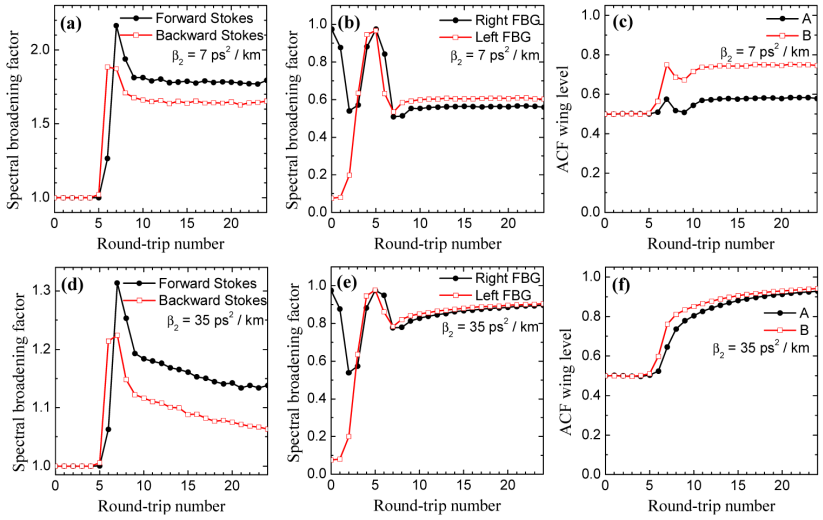

Fig. 3. Spectral broadening in turbulent (upper row, a–c) and laminar (lower row, d–f) regimes. (a), (d) Spectral broadening factors calculated as Γ_B/Γ_A (black line) and Γ_D/Γ_C (red line). (c), (d) The spectral broadening after reflection from the laser mirrors: factor Γ_C/Γ_B is for the right mirror (black), factor as Γ_A/Γ_D is for the left mirror (red). (c), (f) Intensity ACF background level (calculated at large temporal delays) at points A (black) and B (red).

During the first few round-trips, while the radiation exponentially grows from the initial noise, the spectral properties in both regimes are almost the same, and there is no any spectral broadening during the propagation over the fiber, Figs. 3(a)-3(d). At the same time, the mirrors substantially filter out the amplified radiation out of mirrors bandwidth, Figs. 3(b)-

#248319 Received 21 Aug 2015; revised 5 Oct 2015; accepted 6 Oct 2015; published 12 Oct 2015

3(e), see data up to 5th round-trip. After this initial stage the spectral broadening starts. In turbulent case (low dispersion, 7 ps^2/km), the broadening factor tends to be around value of 2, i.e. the spectrum becomes almost twice broader after propagation over fiber comparing to that before the propagation, Fig. 3(b). However, each laser mirror sufficiently filters the radiation making the reflected spectrum almost twice as narrow (Fig. 3(d)) which is in agreement with recent experimental studies [18].

In the laminar case, at larger fiber dispersion, the radiation builds up in a different way. Again, the spectrum of generation wave becomes broader while propagating in the fiber, but the broadening factor in this case is much lower than in the turbulent case, being in the range 1.1–1.3, Fig. 3(a). As a result of narrower spectrum, the narrowing factor after the reflection from the laser mirror is less compared with turbulent case, being around 0.9 only.

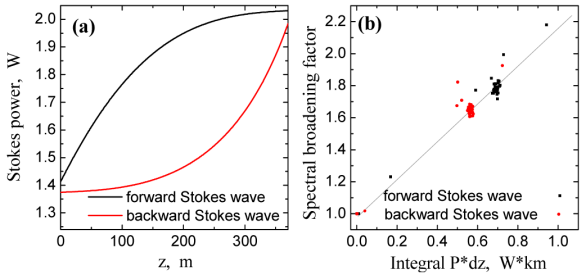

Fig. 4. (a) Longitudinal generation power distribution over the fiber for forward- (black) and backward-propagating (red) generation waves. (b) Linear correlation between spectral broadening factor and integral $\int P(z)\,dz$ for forward (black) and backward propagation wave. Each dot corresponds to one cavity round-trip, gray line shows linear trend.

Note substantially different spectral broadening factors for forward and backward-propagating generation waves (see black and red symbols on Figs. 3(a) and 3(b)), also observed in Ref [18]. Since spectral broadening in both regimes is a nonlinear process, its rate is proportional to the product of wave intensitiy and propagation distance. So overall spectral broadening is determined by integral $\int P\,dz$, which is larger for forward-propagating wave ("+"-wave) due to the pump power depletion (see Fig. 4(a)). Spectral broadening factors Γ_B/Γ_A and Γ_D/Γ_C show strong linear correlation with $\int P\,dz$ (see Fig. 4(b)) with Pearson linear correlation coefficient of 0.98.

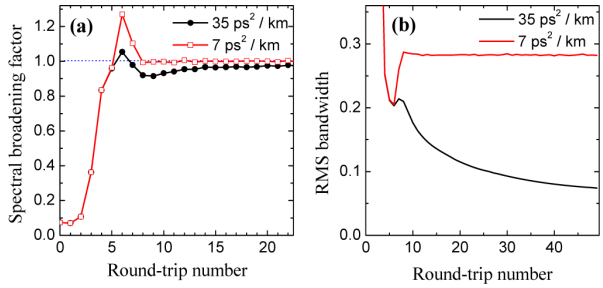

Fig. 5. (a) Total spectral broadening factor calculated over entire cavity round-trip in laminar (black) and turbulent (red) regimes. Horizontal line marks the level at which there is no any spectral broadening or narrowing, i.e. spectral broadening factor is equal to unity. (b) Evolution of rms spectral width in laminar (black) and turbulent (red) regimes.

As a result of subsequent broadening during propagation and spectral narrowing on cavity mirrors, the spectrum acquires the self-sustained form in the case of turbulent generation: the total spectral broadening over the cavity round-trips fluctuates near unity after 7th round-trip, Fig. 5(a). Four-wave mixing induced turbulent spectral broadening in this case is exactly balanced by the narrowing on mirrors. Note that the balance cannot be reached after half of

#248319 Received 21 Aug 2015; revised 5 Oct 2015; accepted 6 Oct 2015; published 12 Oct 2015

cavity round-trip, i.e. after propagation only in one direction and reflection from only one mirror. The total balance over cavity round-trip is important, so the radiation needs to make a full round-trip to reach the equilibrium.

In the laminar regime, the total broadening over the entire cavity round-trip is less than unity, Fig. 5(a), meaning that the spectrum becomes narrower and narrower while radiation continues to be trapped inside the cavity. Overall, a much larger number of round-trips is needed to reach the equilibrium state in the laminar case, Fig. 5(b). It seems that the precise spectral profiles of laser mirrors are important to establish the total balance between spectral broadening during propagation and spectral narrowing on laser mirrors.

Another important question remaining unclear is the role of spectral correlations in both regimes. The spectral correlations should vanish during multiple four-wave mixing processes occurring during the propagation over the fiber. This results in spectral broadening, i.e. in the redistribution of the energy to the far spectral wings. However, each reflection from cavity mirrors removes excess spectral wings and tends to make the radiation less stochastic. In the case of large dispersion, i.e. in the laminar regime, the contribution of four-wave mixing is smaller because of larger dispersion induced mismatch, so specific spectral correlations could potentially sustain during broadening/filtering processes, which leads eventually to the formation of the coherent laminar state. This should be further investigated in details.

The amount of spectral correlations could be phenomenologically taken into account by calculating the background level of the intensity autocorrelation function $K(t) = \left(\int P(\tau)P(t+\tau)\,d\tau\right) \Big/ \left(\int P^2(\tau)\,d\tau\right)$, $K_{bg} = \lim_{t\to\infty} K(t)$, where P is generation power. In turbulent regime, the radiation is almost completely stochastic as K_{bg} = 0.5 (this value corresponds to the exponential statistics for the total intensity, i.e. spectral correlations are absent), Fig. 3(c). Very recently by using a novel asynchronous optical sampling technique, it was experimentally shown that intensity probability density function is almost exponential in a turbulent regime [19]. Note that the radiation co-propagating with the pump wave is less stochastic, as K_{bg} reaches almost 0.8, Fig. 3(c), red curve, i.e. substantial spectral correlations exist. In the laminar regime, the radiation becomes gradually more and more coherent, as K_{bg} gradually increases over cavity passes, Fig. 3(f). Further studies of the evolution of the intensity probability density function and spectral correlation function could provide additional insight on the mechanisms of the laminar and turbulent generation build-up and mechanism of establishing and loss of coherence and spectral correlations in the system.

4. Conclusion

To conclude, the acquired spectrum shape in different generation regime is defined by the balance of the spectral broadening during the propagating over the cavity fiber and spectral narrowing during the reflection from cavity mirrors. In turbulent regime, the overall spectral broadening balance after each round-trip is around unity, which results in establishing the self-similar generation spectrum which is not changed from one round-trip to another. In laminar regime, the radiation becomes gradually narrower at each cavity round-trip as the spectral narrowing prevails over spectral broadening because of specific mirrors spectral profiles and dispersion restricted nonlinear spectral broadening during propagation over the cavity fiber.

Acknowledgments

We acknowledge support by the ERC project UltraLaser, the Russian Ministry of Education and Science (14.B25.31.0003, ZN-06-14/2419), the Russian Foundation for Basic Research (15-02-07925), Presidential Grant for Young researchers (14.120.14.228-MK). N.T. is supported by the Russian Science Foundation (14-21-00110).

#248319 Received 21 Aug 2015; revised 5 Oct 2015; accepted 6 Oct 2015; published 12 Oct 2015